Evidence of a New Narrow Resonance Decaying to $\chi_{c1}\gamma$ in $B \to \chi_{c1}\gamma K$

V. Bhardwaj,[38] K. Miyabayashi,[38] I. Adachi,[13] H. Aihara,[61] D. M. Asner,[46] V. Aulchenko,[3] T. Aushev,[21] T. Aziz,[56]
A. M. Bakich,[55] A. Bala,[47] B. Bhuyan,[15] M. Bischofberger,[38] A. Bondar,[3] G. Bonvicini,[66] A. Bozek,[42] M. Bračko,[31,22]
J. Brodzicka,[42] T. E. Browder,[12] V. Chekelian,[32] A. Chen,[39] B. G. Cheon,[11] K. Chilikin,[21] R. Chistov,[21] K. Cho,[25]
V. Chobanova,[32] S.-K. Choi,[10] Y. Choi,[54] D. Cinabro,[66] J. Dalseno,[32,57] M. Danilov,[21,34] Z. Doležal,[4] Z. Drásal,[4]
A. Drutskoy,[21,34] D. Dutta,[15] K. Dutta,[15] S. Eidelman,[3] D. Epifanov,[3] H. Farhat,[66] J. E. Fast,[46] T. Ferber,[6] A. Frey,[9]
V. Gaur,[56] N. Gabyshev,[3] S. Ganguly,[66] R. Gillard,[66] Y. M. Goh,[11] B. Golob,[29,22] J. Haba,[13] T. Hara,[13] H. Hayashii,[38]
Y. Horii,[37] Y. Hoshi,[59] W.-S. Hou,[41] Y. B. Hsiung,[41] H. J. Hyun,[27] T. Iijima,[37,36] K. Inami,[36] A. Ishikawa,[60] R. Itoh,[13]
T. Iwashita,[38] T. Julius,[33] D. H. Kah,[27] J. H. Kang,[68] E. Kato,[60] T. Kawasaki,[44] H. Kichimi,[13] C. Kiesling,[32] D. Y. Kim,[53]
J. B. Kim,[26] J. H. Kim,[25] K. T. Kim,[26] M. J. Kim,[27] Y. J. Kim,[25] K. Kinoshita,[5] J. Klucar,[22] B. R. Ko,[26] P. Kodyš,[4]
S. Korpar,[31,22] P. Križan,[29,22] P. Krokovny,[3] R. Kumar,[49] T. Kumita,[63] A. Kuzmin,[3] Y.-J. Kwon,[68] J. S. Lange,[7] S.-H. Lee,[26]
J. Li,[52] Y. Li,[65] C. Liu,[51] Z. Q. Liu,[17] D. Liventsev,[13] P. Lukin,[3] D. Matvienko,[3] H. Miyata,[44] R. Mizuk,[21,34]
G. B. Mohanty,[56] A. Moll,[32,57] R. Mussa,[20] E. Nakano,[45] M. Nakao,[13] Z. Natkaniec,[42] M. Nayak,[16] E. Nedelkovska,[32]
N. K. Nisar,[56] S. Nishida,[13] O. Nitoh,[64] S. Ogawa,[58] S. Okuno,[23] S. L. Olsen,[52] P. Pakhlov,[21,34] G. Pakhlova,[21]
E. Panzenböck,[9,38] H. Park,[27] H. K. Park,[27] T. K. Pedlar,[30] R. Pestotnik,[22] M. Petrič,[22] L. E. Piilonen,[65] M. Ritter,[32]
M. Röhrken,[24] A. Rostomyan,[6] H. Sahoo,[12] T. Saito,[60] K. Sakai,[13] Y. Sakai,[13] S. Sandilya,[56] D. Santel,[5] L. Santelj,[22]
T. Sanuki,[60] Y. Sato,[60] V. Savinov,[48] O. Schneider,[28] G. Schnell,[1,14] C. Schwanda,[18] R. Seidl,[50] D. Semmler,[7] K. Senyo,[67]
O. Seon,[36] M. E. Sevior,[33] M. Shapkin,[19] C. P. Shen,[36] T.-A. Shibata,[62] J.-G. Shiu,[41] B. Shwartz,[3] F. Simon,[32,57]
J. B. Singh,[47] P. Smerkol,[22] Y.-S. Sohn,[68] A. Sokolov,[19] E. Solovieva,[21] M. Starič,[22] M. Steder,[6] M. Sumihama,[8]
T. Sumiyoshi,[63] U. Tamponi,[20] K. Tanida,[52] G. Tatishvili,[46] Y. Teramoto,[45] K. Trabelsi,[13] T. Tsuboyama,[13] M. Uchida,[62]
S. Uehara,[13] T. Uglov,[21,35] Y. Unno,[11] P. Urquijo,[2] Y. Usov,[3] S. E. Vahsen,[12] C. Van Hulse,[1] P. Vanhoefer,[32] G. Varner,[12]
K. E. Varvell,[55] A. Vinokurova,[3] M. N. Wagner,[7] C. H. Wang,[40] M.-Z. Wang,[41] P. Wang,[17] M. Watanabe,[44] Y. Watanabe,[23]
E. Won,[26] B. D. Yabsley,[55] J. Yamaoka,[12] Y. Yamashita,[43] S. Yashchenko,[6] Y. Yook,[68] C. Z. Yuan,[17] C. C. Zhang,[17]
Z. P. Zhang,[51] V. Zhilich,[3] V. Zhulanov,[3] and A. Zupanc[24]

(Belle Collaboration)

[1]*University of the Basque Country UPV/EHU, 48080 Bilbao*
[2]*University of Bonn, 53115 Bonn*
[3]*Budker Institute of Nuclear Physics SB RAS and Novosibirsk State University, Novosibirsk 630090*
[4]*Faculty of Mathematics and Physics, Charles University, 121 16 Prague*
[5]*University of Cincinnati, Cincinnati, Ohio 45221*
[6]*Deutsches Elektronen–Synchrotron, 22607 Hamburg*
[7]*Justus-Liebig-Universität Gießen, 35392 Gießen*
[8]*Gifu University, Gifu 501-1193*
[9]*II. Physikalisches Institut, Georg-August-Universität Göttingen, 37073 Göttingen*
[10]*Gyeongsang National University, Chinju 660-701*
[11]*Hanyang University, Seoul 133-791*
[12]*University of Hawaii, Honolulu, Hawaii 96822*
[13]*High Energy Accelerator Research Organization (KEK), Tsukuba 305-0801*
[14]*Ikerbasque, 48011 Bilbao*
[15]*Indian Institute of Technology Guwahati, Assam 781039*
[16]*Indian Institute of Technology Madras, Chennai 600036*
[17]*Institute of High Energy Physics, Chinese Academy of Sciences, Beijing 100049*
[18]*Institute of High Energy Physics, Vienna 1050*
[19]*Institute for High Energy Physics, Protvino 142281*
[20]*INFN - Sezione di Torino, 10125 Torino*
[21]*Institute for Theoretical and Experimental Physics, Moscow 117218*
[22]*J. Stefan Institute, 1000 Ljubljana*
[23]*Kanagawa University, Yokohama 221-8686*
[24]*Institut für Experimentelle Kernphysik, Karlsruher Institut für Technologie, 76131 Karlsruhe*
[25]*Korea Institute of Science and Technology Information, Daejeon 305-806*
[26]*Korea University, Seoul 136-713*
[27]*Kyungpook National University, Daegu 702-701*

^{28}École Polytechnique Fédérale de Lausanne (EPFL), Lausanne 1015

^{29}Faculty of Mathematics and Physics, University of Ljubljana, 1000 Ljubljana

^{30}Luther College, Decorah, Iowa 52101

^{31}University of Maribor, 2000 Maribor

^{32}Max-Planck-Institut für Physik, 80805 München

^{33}School of Physics, University of Melbourne, Victoria 3010

^{34}Moscow Physical Engineering Institute, Moscow 115409

^{35}Moscow Institute of Physics and Technology, Moscow Region 141700

^{36}Graduate School of Science, Nagoya University, Nagoya 464-8602

^{37}Kobayashi-Maskawa Institute, Nagoya University, Nagoya 464-8602

^{38}Nara Women's University, Nara 630-8506

^{39}National Central University, Chung-li 32054

^{40}National United University, Miao Li 36003

^{41}Department of Physics, National Taiwan University, Taipei 10617

^{42}H. Niewodniczanski Institute of Nuclear Physics, Krakow 31-342

^{43}Nippon Dental University, Niigata 951-8580

^{44}Niigata University, Niigata 950-2181

^{45}Osaka City University, Osaka 558-8585

^{46}Pacific Northwest National Laboratory, Richland, Washington 99352

^{47}Panjab University, Chandigarh 160014

^{48}University of Pittsburgh, Pittsburgh, Pennsylvania 15260

^{49}Punjab Agricultural University, Ludhiana 141004

^{50}RIKEN BNL Research Center, Upton, New York 11973

^{51}University of Science and Technology of China, Hefei 230026

^{52}Seoul National University, Seoul 151-742

^{53}Soongsil University, Seoul 156-743

^{54}Sungkyunkwan University, Suwon 440-746

^{55}School of Physics, University of Sydney, New South Wales 2006

^{56}Tata Institute of Fundamental Research, Mumbai 400005

^{57}Excellence Cluster Universe, Technische Universität München, 85748 Garching

^{58}Toho University, Funabashi 274-8510

^{59}Tohoku Gakuin University, Tagajo 985-8537

^{60}Tohoku University, Sendai 980-8578

^{61}Department of Physics, University of Tokyo, Tokyo 113-0033

^{62}Tokyo Institute of Technology, Tokyo 152-8550

^{63}Tokyo Metropolitan University, Tokyo 192-0397

^{64}Tokyo University of Agriculture and Technology, Tokyo 184-8588

^{65}CNP, Virginia Polytechnic Institute and State University, Blacksburg, Virginia 24061

^{66}Wayne State University, Detroit, Michigan 48202

^{67}Yamagata University, Yamagata 990-8560

^{68}Yonsei University, Seoul 120-749

We report measurements of $B \to \chi_{c1}\gamma K$ and $\chi_{c2}\gamma K$ decays using 772×10^6 $B\bar{B}$ events collected at the $\Upsilon(4S)$ resonance with the Belle detector at the KEKB asymmetric-energy e^+e^- collider. Evidence of a new resonance in the $\chi_{c1}\gamma$ final state is found with a statistical significance of 3.8σ. This state has a mass of $3823.1 \pm 1.8(\text{stat}) \pm 0.7(\text{syst})$ MeV/c^2, a value that is consistent with theoretical expectations for the previously unseen 1^3D_2 $c\bar{c}$ meson. We find no other narrow resonance and set upper limits on the branching fractions of the $X(3872) \to \chi_{c1}\gamma$ and $\chi_{c2}\gamma$ decays.

During the last decade, a number of new charmonium ($c\bar{c}$)-like states were observed, many of which are candidates for exotic states [1]. The first of these, the $X(3872)$, has been observed by six different experiments in the same final state [2–7]. A recent update from the Belle [8] and LHCb [6] Collaborations results in a world average mass at 3871.68 ± 0.17 MeV/c^2 [9] and a stringent upper bound on its width ($\Gamma < 1.2$ MeV) [8]. The proximity of its mass to the $D^{*0}\bar{D}^0$ threshold makes it a good candidate for a $D\bar{D}^*$ molecule [10]. Other alternative models have been proposed, such as a tetraquark [11] or a $c\bar{c}g$ hybrid meson [12].

Radiative decays can illuminate clearly the nature of hadrons. For example, the observation of $X(3872) \to J/\psi\gamma$

confirmed the C-even parity assignment for the $X(3872)$ [13,14]. The $X(3872) \rightarrow \chi_{c1}\gamma$ and $\chi_{c2}\gamma$ decays are forbidden by C-parity conservation in electromagnetic processes. However, if the $X(3872)$ is a tetraquark or a molecular state, it may have a C-odd partner, which could decay into $\chi_{c1}\gamma$ and $\chi_{c2}\gamma$ final states [15,16].

In the charmonium family, the observation of a D-wave $c\bar{c}$ meson and its decay modes would test phenomenological models [17,18]. The as-yet undiscovered $1^3D_2 c\bar{c}$ (ψ_2) and $1^3D_3 c\bar{c}(\psi_3)$ states are expected to have significant branching fractions to $\chi_{c1}\gamma$ and $\chi_{c2}\gamma$, respectively [19,20]. D-wave $c\bar{c}$ states and their properties were predicted long ago but remain unconfirmed [19,20]. The E705 experiment reported an indication of a 1^3D_2 state in $\pi^{\pm}N \rightarrow J/\psi\pi^+\pi^- +$ anything, with a mass of 3836 ± 13 MeV/c^2 [21]; however, the statistical significance of this result was below the threshold for evidence.

In this Letter, we report measurements of $B \rightarrow \chi_{c1}\gamma K$ and $B \rightarrow \chi_{c2}\gamma K$ decays, where the χ_{c1} and χ_{c2} decay to $J/\psi\gamma$ [22]. These results are obtained from a data sample of 772×10^6 $B\bar{B}$ events collected with the Belle detector [23] at the KEKB asymmetric-energy e^+e^- collider operating at the $\Upsilon(4S)$ resonance [24].

The J/ψ meson is reconstructed via its decays to $\ell^+\ell^-$ ($\ell = e$ or μ). To reduce the radiative tail in the e^+e^- mode, the four-momenta of all photons within 50 mrad with respect to the original direction of the e^+ or e^- tracks are included in the invariant mass calculation, hereinafter denoted as $M_{e^+e^-(\gamma)}$. The reconstructed invariant mass of the J/ψ candidates is required to satisfy 2.95 GeV/$c^2 <$ $M_{e^+e^-(\gamma)} < 3.13$ GeV/c^2 or 3.03 GeV/$c^2 < M_{\mu^+\mu^-} <$ 3.13 GeV/c^2. For the selected J/ψ candidates, a vertex-constrained fit is applied and then a mass-constrained fit is performed in order to improve the momentum resolution. The χ_{c1} and χ_{c2} candidates are reconstructed by combining J/ψ candidates with a photon having energy (E_γ) larger than 200 MeV in the laboratory frame. Photons are reconstructed from energy depositions in the electromagnetic calorimeter, which do not match any extrapolated charged track. To reduce the background from $\pi^0 \rightarrow \gamma\gamma$, we use a likelihood function that distinguishes an isolated photon from π^0 decays using the photon pair invariant mass, photon laboratory energy, and polar angle [25]. We reject both γ's in the pair if the π^0 likelihood probability is larger than 0.7. The reconstructed invariant mass of the χ_{c1} (χ_{c2}) is required to satisfy 3.467 GeV/$c^2 < M_{J/\psi\gamma} <$ 3.535 GeV/c^2 (3.535 GeV/$c^2 < M_{J/\psi\gamma} < 3.611$ GeV/c^2). A mass-constrained fit is applied to the selected χ_{c1} and χ_{c2} candidates.

Charged kaons are identified by combining information from the central drift chamber, time-of-flight scintillation counters, and the aerogel Cherenkov counter systems. The kaon identification efficiency is 89% while the probability of misidentifying a pion as a kaon is 10%. K_S^0 mesons are reconstructed by combining two oppositely charged pions

with the invariant mass $M_{\pi^+\pi^-}$ lying between 482 and 514 MeV/c^2. The selected candidates are required to satisfy the quality criteria described in Ref. [26].

To reconstruct B candidates, each χ_{cJ} [27] is combined with a kaon candidate and a photon having $E_\gamma > 100$ MeV (and not used in the reconstruction of χ_{cJ}). If the invariant mass of any photon pair that includes this photon is found to be consistent with a π^0 (i.e., 117 MeV/$c^2 < M_{\gamma\gamma} <$ 153 MeV/c^2), this photon is rejected. Among the events containing at least one χ_{cJ} candidate, 9.0% have multiple χ_{cJ} candidates. In such cases, the γ forming the χ_{cJ} candidate with mass closest to the χ_{c1} or χ_{c2} masses [9] is not used as the additional photon. This treatment suppresses reflections from the χ_{cJ} daughter photons.

The B candidate is identified by two kinematic variables: the beam-constrained mass ($M_{\rm bc} \equiv \sqrt{E_{\rm beam}^{*2} - p_B^{*2}}$) and the energy difference ($\Delta E \equiv E_B^* - E_{\rm beam}^*$). Here, $E_{\rm beam}^*$ is the run-dependent beam energy, and E_B^* and p_B^* are the reconstructed energy and momentum, respectively, of the B meson candidates in the center-of-mass frame. Candidates within a ΔE window of [-28, 30] MeV and with $M_{\rm bc} > 5.23$ GeV/c^2 are selected. Of these, 9.8% (6.4%) have multiple candidates in the $B^{\pm} \rightarrow \chi_{c1}\gamma K^{\pm}$ ($B^{\pm} \rightarrow \chi_{c2}\gamma K^{\pm}$) mode; we select the B candidate with ΔE closest to zero. In order to improve the resolution in $M_{\chi_{cJ}\gamma}$, we scale the energy of the γ so that ΔE is equal to zero. This corrects for incomplete energy measurement in the electromagnetic calorimeter. To suppress continuum background, events having a ratio R_2 of the second to zeroth Fox-Wolfram moments [28] above 0.5 are rejected.

The $M_{\chi_{c1}\gamma}$ and $M_{\rm bc}$ projections for the $B^{\pm} \rightarrow \chi_{c1}\gamma K^{\pm}$ signal candidates are shown in Fig. 1, where a $\psi' \rightarrow \chi_{c1}\gamma$ signal is evident. In addition, there is a significant narrow peak at 3823 MeV/c^2, denoted hereinafter as $X(3823)$. No signal of $X(3872) \rightarrow \chi_{c1}\gamma$ is seen. We extract the signal yield from a two-dimensional unbinned extended maximum likelihood (2D UML) fit to the variables $M_{\chi_{cJ}\gamma}$ and $M_{\rm bc}$.

The resolution in $M_{\chi_{cJ}\gamma}$ ($M_{\rm bc}$) is parametrized by a sum of two Gaussians (Gaussian and logarithmic Gaussian [29]). Monte Carlo (MC) studies show that the resolutions in both $M_{\chi_{cJ}\gamma}$ and $M_{\rm bc}$ for a narrow resonance in the mass range 3.8 GeV/$c^2 < M_{\chi_{cJ}\gamma} < 4.0$ GeV/c^2 are in good agreement with those for ψ'. The parameters of the resolution functions are determined from the MC simulation that is calibrated using the $B^{\pm} \rightarrow \psi'(\rightarrow \chi_{c1}\gamma)K^{\pm}$ signal. We take into account the ψ' natural width [9] by convolving the Breit-Wigner function and the resolution function; for the $X(3823)$ and $X(3872)$, zero natural widths are assumed. The two-dimensional probability density function (PDF) is a product of the one-dimensional distributions.

For $B^{\pm} \rightarrow \psi'(\rightarrow \chi_{c1}\gamma)K^{\pm}$ decays, the mean and width of the core Gaussian are floated and the remaining
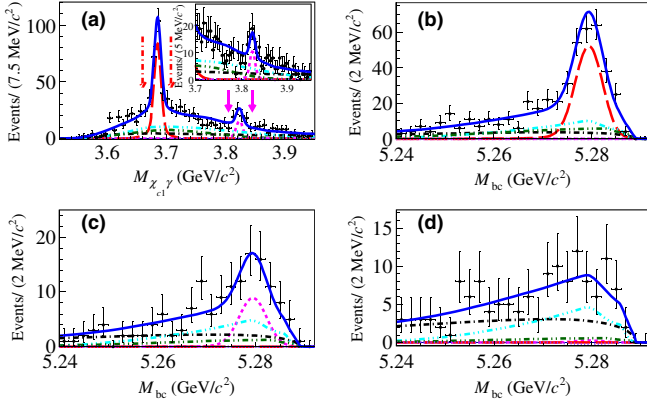
FIG. 1 (color online). 2D UML fit projection for $B^{\pm} \rightarrow (\chi_{c1}\gamma)K^{\pm}$ decays: (a) $M_{\chi_{c1}\gamma}$ distribution for $M_{bc} > 5.27$ GeV/c^2, (b) M_{bc} distribution for 3.660 GeV/$c^2 < M_{\chi_{c1}\gamma} < 3.708$ GeV/c^2 [ψ' region, shown by the dot-dashed red arrows in (a)], (c) M_{bc} distribution for 3.805 GeV/$c^2 < M_{\chi_{c1}\gamma} < 3.845$ GeV/c^2 [$X(3823)$ region, shown by the solid magenta arrows in (a)], and (d) M_{bc} distribution for 3.84 GeV/$c^2 < M_{\chi_{c1}\gamma} < 3.89$ GeV/c^2 [$X(3872)$ region]. The curves used in the fits are described in Ref. [40].
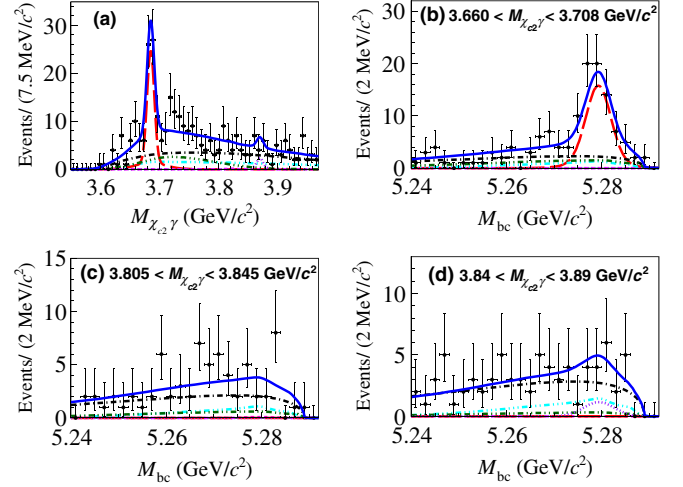

FIG. 2 (color online). 2D UML fit projection for $B^{\pm} \rightarrow (\chi_{c2}\gamma)K^{\pm}$ decays: (a) $M_{\chi_{c2}\gamma}$ distribution for $M_{bc} > 5.27$ GeV/c^2, (b) M_{bc} distribution for the ψ' region, (c) M_{bc} distribution for the $X(3823)$ region, and (d) M_{bc} distribution for the $X(3872)$ region. The curves used in the fits are described in Ref. [40].

parameters are fixed according to MC simulations. To fit the $B^{\pm} \rightarrow X(3823)(\rightarrow \chi_{c1}\gamma)K^{\pm}$ signal, we float the mean of the core Gaussian but constrain the detector resolution by using the ψ' signal results after taking into account the difference estimated from the signal MC study. For M_{bc}, the parameters are fixed to those found for the ψ', in accordance with expectations based on the MC simulation. For $X(3872)$, we fix the mass difference and the mass resolution change with respect to ψ' using the information from Particle Data Group (PDG) [9] and MC studies. To fit $B^0 \rightarrow \psi'(\rightarrow \chi_{c1}\gamma)K^0$, $B^0 \rightarrow X(3823)(\rightarrow \chi_{c1}\gamma)K^0$, $B \rightarrow \psi'(\rightarrow \chi_{c2}\gamma)K$, $B \rightarrow X(3823)(\rightarrow \chi_{c2}\gamma)K$, and $B \rightarrow X(3872)(\rightarrow \chi_{cJ}\gamma)K$, we fix all the parameters obtained from the signal MC study after correcting the PDF shapes by applying MC-data calibration factors.

To study background with a real J/ψ, we use large MC simulated $B \rightarrow J/\psi X$ samples corresponding to 100 times the integrated luminosity of the data. The non-J/ψ (non-χ_{cJ}) background is studied using $M_{\ell\ell}$ ($M_{J/\psi\gamma}$) sidebands in data. In $B \rightarrow (\chi_{cJ}\gamma)K$, the background with a broad peaking structure is mostly due to the $B \rightarrow \psi'(\nrightarrow \chi_{cJ}\gamma)K$, $B \rightarrow \chi_{cJ}K^*$, $B \rightarrow J/\psi K^*$, and $B \rightarrow \psi'K^*$ decay modes. $B \rightarrow \psi'(\nrightarrow \chi_{cJ}\gamma)K$ produces peaks in both distributions ($M_{\chi_{cJ}\gamma}$ and M_{bc}), while the other backgrounds are flat in $M_{\chi_{cJ}\gamma}$ but peaked in M_{bc}. We determine the PDFs from the large MC sample. The fractions of the PDF components are floated in the fit, except for $B \rightarrow \psi'(\nrightarrow \chi_{cJ}\gamma)K$, whose fraction is controlled by fixing its ratio to the $B \rightarrow \psi'(\rightarrow \chi_{cJ}\gamma)K$ signal yield. For the combinatorial background, a threshold function $(M_{\chi_{cJ}\gamma})^2 \times \exp[a(M_{\chi_{cJ}\gamma} - M_{th}) + b(M_{\chi_{cJ}\gamma} - M_{th})^2 + c(M_{\chi_{cJ}\gamma} - M_{th})^3]$, where $M_{th} = 3.543$ GeV/c^2

(3.585 GeV/c^2) for $M_{\chi_{c1}\gamma}$ ($M_{\chi_{c2}\gamma}$), is used for $M_{\chi_{cJ}\gamma}$, and an ARGUS function [30] is used for M_{bc}. The value of M_{th} is estimated from a MC study; its variation, which affects the signal yield in the fits, is incorporated in the systematic errors. The ΔE data sidebands are used to verify the background PDFs. The fractions for the signal and the background components are floated in the fit.

The results of the fits are presented in Figs. 1–3 and in Table I. The significance is estimated using the value of $-2\ln(\mathcal{L}_0/\mathcal{L}_{max})$, where $\mathcal{L}_{max}$ ($\mathcal{L}_0$) denotes the likelihood value when the yield is allowed to vary (is set to zero). In the likelihood calculation, the χ^2 statistic uses the appropriate number of degrees of freedom [two in the case of $B^{\pm} \rightarrow X(3823)K^{\pm}$ and one for the other decay modes]. The systematic uncertainty, which is described below, is included in the significance calculation [31]. We find a significant ψ' signal in all considered channels. We also obtain evidence for the $X(3823)$ in the channel $B^{\pm} \rightarrow \chi_{c1}\gamma K^{\pm}$ with a statistical significance of 3.8 standard deviations (σ). The $X(3872)$ signals are insignificant. We estimate the branching fractions according to the formula $\mathcal{B} = Y/(\epsilon \mathcal{B}_s N_{B\bar{B}})$; here, Y is the yield, ϵ is the reconstruction efficiency, $\mathcal{B}_s$ is the secondary branching fraction taken from Ref. [9], and $N_{B\bar{B}}$ is the number of $B\bar{B}$ mesons in the data sample. Equal production of neutral and charged B meson pairs in the $\Upsilon(4S)$ decay is assumed. Measured branching fractions for the ψ' are in agreement with the world average values for all the channels [9]. We set 90% confidence level (C.L.) upper limits (U.L.) on the insignificant channels using frequentist methods based on an ensemble of pseudoexperiments.

A correction for small differences in the signal detection efficiency between MC simulations and data has been
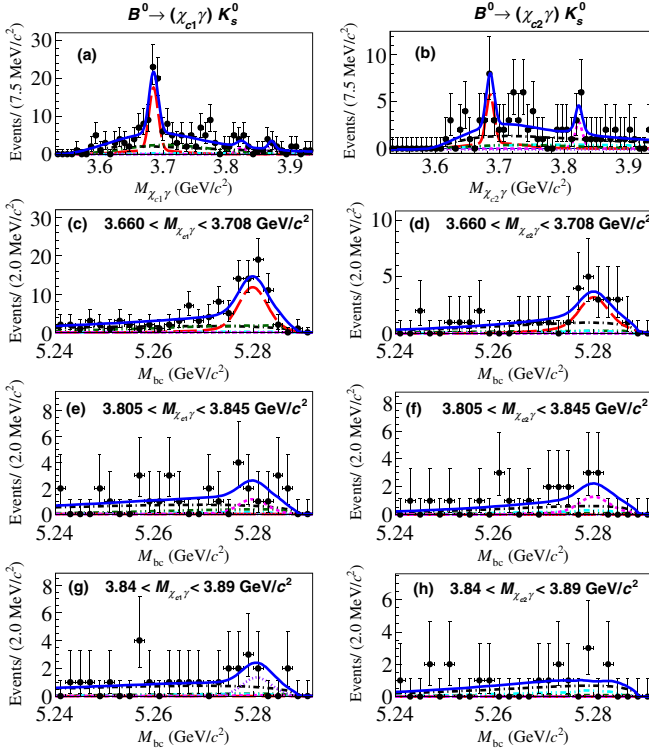
FIG. 3 (color online). 2D UML fit projection for $B^0 \to (\chi_{cJ}\gamma)K_S^0$ decays: (a) $M_{\chi_{c1}\gamma}$ distribution for $M_{bc} > 5.27$ GeV/c^2; (b) $M_{\chi_{c2}\gamma}$ distribution for $M_{bc} > 5.27$ GeV/c^2; (c), (d) M_{bc} distribution for the ψ' region; (e), (f) M_{bc} distribution for the $X(3823)$ region; and (g), (h) M_{bc} distribution for the $X(3872)$ region. The curves used in the fits are described in Ref. [40].

applied for the lepton and kaon identification requirements. Uncertainties in these corrections are included in the systematic error. The $e^+ e^- \to e^+ e^- \ell^+ \ell^-$ ($\ell = e$ or μ) and $D^{*+} \to D^0(K^-\pi^+)\pi^+$ samples are used to estimate the lepton identification correction and the kaon (pion) identification correction, respectively. To estimate the correction and residual systematic uncertainty for K_S^0 reconstruction, $D^{*+} \to D^0(\to K_S^0\pi^+\pi^-)\pi^+$ samples are used. The errors on the PDF shapes are obtained by varying all fixed parameters by $\pm 1\sigma$ and taking the change in the yield as the systematic uncertainty. The uncertainties due to the secondary branching fractions are also taken into account. The uncertainties of the tracking efficiency and $N_{B\bar{B}}$ are estimated to be 0.35% per track and 1.4%, respectively. The uncertainty on the photon identification is estimated to be 2.0%/photon. The systematic uncertainty associated with the difference of the π^0 veto between data and MC simulation is estimated to be 1.2% from a study of the $B^\pm \to \chi_{c1}(\to J/\psi\gamma)K^\pm$ sample.

To improve the mass determination of the $X(3823)$, a simultaneous fit to $B^\pm \to (\chi_{c1}\gamma)K^\pm$ and $B^0 \to (\chi_{c1}\gamma)K_S^0$ is performed, assuming that $\mathcal{B}(B^\pm \to X(3823)K^\pm)/\mathcal{B}(B^0 \to X(3823)K^0) = \mathcal{B}(B^\pm \to \psi'K^\pm)/\mathcal{B}(B^0 \to \psi'K^0)$. The ψ' peak position and $M_{\chi_{c1}\gamma}$ resolution are common for

both charged and neutral B candidates. From this fit (shown in Fig. 4), we estimate the significance for $X(3823)$ to be 4.0σ (including systematic uncertainties). We determine the mass of the signal peak relative to the well-measured ψ' mass:

$$M_{X(3823)} = M_{X(3823)}^{\text{meas}} - M_{\psi'}^{\text{meas}} + M_{\psi'}^{\text{PDG}}$$
$$= 3823.1 \pm 1.8 \pm 0.7 \text{ MeV}.$$

Here, the first uncertainty is statistical and the second is systematic. Because of the mass-constrained fit to the χ_{c1} candidate, the systematic uncertainty of $M_{X(3823)}$ is dominated by the additional photon's energy scale. This photon energy scale uncertainty is estimated by the difference between the $\chi_{c1} \to J/\psi\gamma$ candidates' mass without any constraint and the χ_{c1} nominal mass [9], which results in 0.7 MeV as the $M_{X(3823)}$ systematic error. In order to estimate the width, we float this parameter and find no sensitivity with the available statistics: the width is 1.7 ± 5.5 MeV. Using pseudoexperiments generated with different width hypotheses for the $X(3823)$, the U.L. at 90% C.L. on its width is estimated to be 24 MeV.

The mass of the $X(3823)$ is near potential model expectations for the centroid of the 1^3D_J states: the Cornell [17] and the Buchmüller-Tye [18] potentials give 3810 MeV/c^2. Other models predict the mass of ψ_2 (the $1^3D_2 c\bar{c}$ state, having $J^{PC} = 2^{--}$) to be 3815–3840 MeV/c^2 [32–35]. The $X(3823)$ mass agrees

TABLE I. Summary of the results. Signal yield (Y) from the fit, significance ($\mathcal{S}$) with systematics included, corrected efficiency (ϵ), and measured $\mathcal{B}$. For $\mathcal{B}$, the first (second) error is statistical (systematic). In the neutral B decay, the efficiency below includes the $K_S^0 \to \pi^+\pi^-$ branching fraction but does not include the factor of two for $K^0 \to K_S^0$ or K_L^0.

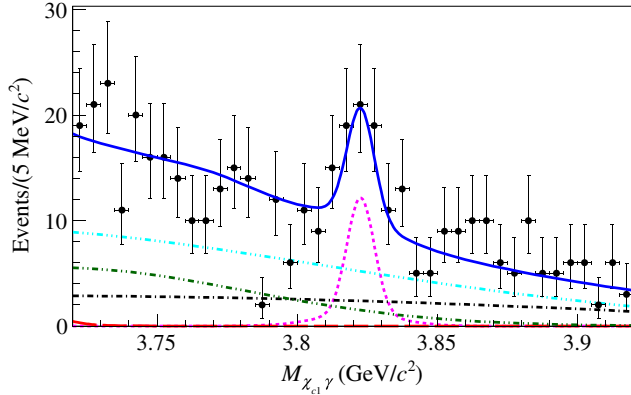| Decay	Yield (Y)	$\mathcal{S}(\sigma)$	$\epsilon(\%)$	Branching fraction
$B^\pm \to \psi'(\to \chi_{cJ}\gamma)K^\pm$				$\mathcal{B}(10^{-4})$
χ_{c1}	193.2 ± 19.2	14.8	8.6	$7.7 \pm 0.8 \pm 0.9$
χ_{c2}	59.1 ± 8.4	7.8	6.0	$6.3 \pm 0.9 \pm 0.6$
$B^0 \to \psi'(\to \chi_{cJ}\gamma)K^0$				
χ_{c1}	50.3 ± 7.3	7.2	5.1	$6.8 \pm 1.0 \pm 0.7$
χ_{c2}	12.9 ± 4.4	2.9	3.5	$4.7 \pm 1.6 \pm 0.8$
$B^\pm \to X(3823)(\to \chi_{cJ}\gamma)K^\pm$				$\mathcal{B}(10^{-6})$
χ_{c1}	33.2 ± 9.7	3.8	10.9	$9.7 \pm 2.8 \pm 1.1$
χ_{c2}	0.3 ± 3.9	0.1	8.8	<3.6
$B^0 \to X(3823)(\to \chi_{cJ}\gamma)K^0$				
χ_{c1}	3.9 ± 3.4	1.2	6.0	<9.9
χ_{c2}	5.3 ± 2.9	2.4	5.0	<22.8
$B^\pm \to X(3872)(\to \chi_{cJ}\gamma)K^\pm$				
χ_{c1}	-0.9 ± 5.1		11.1	<1.9
χ_{c2}	4.7 ± 4.4	1.3	9.3	<6.7
$B^0 \to X(3872)(\to \chi_{cJ}\gamma)K^0$				
χ_{c1}	4.6 ± 3.0	1.6	6.2	<9.6
χ_{c2}	2.3 ± 2.2	1.1	5.2	<12.2

FIG. 4 (color online). 2D UML fit projection of the $M_{\chi_{c1}\gamma}$ distribution for the simultaneous fit of $B^{\pm} \rightarrow (\chi_{c1}\gamma)K^{\pm}$ and $B^0 \rightarrow (\chi_{c1}\gamma)K_S^0$ decays for $M_{bc} > 5.27$ GeV/c^2. The curves used in the fits are described in Ref. [40].

quite well with these models. In addition, since no peak has been seen around $X(3823)$ in the $D\bar{D}$ final state [36], one expects that ψ_2 does not decay to $D\bar{D}$ [34]. The ratio $R_B = (\mathcal{B}[X(3823) \rightarrow \chi_{c2}\gamma]/\mathcal{B}[X(3823) \rightarrow \chi_{c1}\gamma]) <$ 0.41 (at 90% C.L.) is consistent with the expectation ($R_B \sim 0.2$) for ψ_2 [33,37,38]. The limited statistics preclude an angular analysis to determine the J^{PC} of the $X(3823)$. The product of branching fractions for the $X(3823)$ is approximately 2 orders of magnitude lower than for the ψ', as shown in Table I; it is consistent with the interpretation of the $X(3823)$ as $\psi_2(1^3D_2)$, whose production rate is suppressed by the factorization [39] in the two-body B meson decays.

In summary, we obtain the first evidence of a narrow state $X(3823)$ that decays to $\chi_{c1}\gamma$ with a mass of $3823.1 \pm 1.8(\text{stat}) \pm 0.7(\text{syst})$ MeV/c^2 and a significance of 3.8σ, including systematic uncertainties. We measure the branching fraction product $\mathcal{B}[B^{\pm} \rightarrow X(3823)K^{\pm}]\mathcal{B}[X(3823) \rightarrow \chi_{c1}\gamma] = (9.7 \pm 2.8 \pm 1.1) \times 10^{-6}$. No evidence is found for $X(3823) \rightarrow \chi_{c2}\gamma$, and we set an U.L. on its branching fraction product $\mathcal{B}$ as well as the ratio $R_B \equiv (\mathcal{B}[X(3823) \rightarrow \chi_{c2}\gamma]/\mathcal{B}[X(3823) \rightarrow \chi_{c1}\gamma]) < 0.41$ at 90% C.L. The properties of the $X(3823)$ are consistent with those expected for the $\psi_2(1^3D_2 c\bar{c})$ state. We also determine an U.L. on the product of branching fractions $\mathcal{B}[B^{\pm} \rightarrow X(3872)K^{\pm}]\mathcal{B}[X(3872) \rightarrow \chi_{c1}\gamma] < 1.9 \times 10^{-6}$ at 90% C.L.; this is less than one quarter of the corresponding value in $X(3872) \rightarrow J/\psi\pi^+\pi^-$ [9]. Our results show that the production of the $X(3872)$'s C-odd partner in two-body B decays and its decay to $\chi_{cJ}\gamma$ are considerably suppressed.

[1] N. Brambilla et al., Eur. Phys. J. C **71**, 1534 (2011).
[2] S.-K. Choi et al. (Belle Collaboration), Phys. Rev. Lett. **91**, 262001 (2003).
[3] D. Acosta et al. (CDF Collaboration), Phys. Rev. Lett. **93**, 072001 (2004).
[4] V. M. Abazov et al. (D0 Collaboration), Phys. Rev. Lett. **93**, 162002 (2004).
[5] B. Aubert et al. (BABAR Collaboration), Phys. Rev. D **71**, 071103 (2005).
[6] R. Aaij et al. (LHCb Collaboration), Eur. Phys. J. C **72**, 1972 (2012).
[7] V. Chiochia et al. (CMS Collaboration), arXiv:1201.6677.
[8] S.-K. Choi et al. (Belle Collaboration), Phys. Rev. D **84**, 052004 (2011).
[9] J. Beringer et al. (Particle Data Group), Phys. Rev. D **86**, 010001 (2012).
[10] E. S. Swanson, Phys. Lett. B **598**, 197 (2004); Phys. Rep. **429**, 243 (2006).
[11] L. Maiani, F. Piccinini, A. D. Polosa, and V. Riquer, Phys. Rev. D **71**, 014028 (2005).
[12] B. A. Li, Phys. Lett. B **605**, 306 (2005).
[13] B. Aubert et al. (BABAR Collaboration), Phys. Rev. Lett. **102**, 132001 (2009).
[14] V. Bhardwaj et al. (Belle Collaboration), Phys. Rev. Lett. **107**, 091803 (2011).
[15] K. Terasaki, Prog. Theor. Phys. **127**, 577 (2012).
[16] J. Nieves and M. Pavon Valderrama, Phys. Rev. D **86**, 056004 (2012).
[17] E. Eichten, K. Gottfried, T. Kinoshita, K. D. Lane, and T. M. Yan, Phys. Rev. D **17**, 3090 (1978); Phys. Rev. D **21**, 203 (1980).
[18] W. Buchmüller and S.-H. H. Tye, Phys. Rev. D **24**, 132 (1981).
[19] E. J. Eichten, K. Lane, and C. Quigg, Phys. Rev. Lett. **89**, 162002 (2002).
[20] P. Cho and M. B. Wise, Phys. Rev. D **51**, 3352 (1995).
[21] L. Antoniazzi et al. (E705 Collaboration), Phys. Rev. D **50**, 4258 (1994). Note that no hint of the $\psi(3836)$ is seen in $J/\psi\pi^+\pi^-$ studies focused on the $X(3872)$ [2–7].
[22] Charge-conjugate and neutral modes are included throughout the Letter unless stated otherwise.
[23] A. Abashian et al. (Belle Collaboration), Nucl. Instrum. Methods Phys. Res., Sect. A **479**, 117 (2002); also see the detector section in J. Brodzicka et al., Prog. Theor. Exp. Phys. 04D001 (**2012**).
[24] S. Kurokawa and E. Kikutani, Nucl. Instrum. Methods Phys. Res., Sect. A **499**, 1 (2003), and other papers

included in this volume; T. Abe *et al.*, Prog. Theor. Exp. Phys. 03A001 (**2013**) and following articles up to 03A011.

[25] P. Koppenburg *et al.* (Belle Collaboration), Phys. Rev. Lett. **93**, 061803 (2004).

[26] K.-F. Chen *et al.* (Belle Collaboration), Phys. Rev. D **72**, 012004 (2005).

[27] Hereinafter, χ_{cJ} refers to either χ_{c1} or χ_{c2}, depending on which is reconstructed.

[28] G. C. Fox and S. Wolfram, Phys. Rev. Lett. **41**, 1581 (1978).

[29] The logarithmic Gaussian is parametrized as $f(x) = (N_0/[\sqrt{2\pi}\sigma_0(\epsilon - x)])\exp-[(\ln[(\epsilon - x)/(\epsilon - x_p)])^2/(2\sigma_0^2)]$, where $\epsilon = \sigma/a + x_p$ and $\sigma_0 = [\ln(a\sqrt{2\ln 2} + \sqrt{1 + 2a^2 \ln 2})]/\sqrt{2\ln 2}$. Here, N_0 is the normalization, σ is the standard deviation, x_p is the mean, and a is the asymmetry.

[30] H. Albrecht *et al.* (ARGUS Collaboration), Phys. Lett. B **241**, 278 (1990).

[31] R. D. Cousins and V. L. Highland, Nucl. Instrum. Methods Phys. Res., Sect. A **320**, 331 (1992).

[32] S. Godfrey and N. Isgur, Phys. Rev. D **32**, 189 (1985).

[33] D. Ebert, R. N. Faustov, and V. O. Galkin, Phys. Rev. D **67**, 014027 (2003).

[34] E. J. Eichten, K. Lane, and C. Quigg, Phys. Rev. D **69**, 094019 (2004).

[35] M. Blank and A. Krassnigg, Phys. Rev. D **84**, 096014 (2011).

[36] P. Pakhlov *et al.* (Belle Collaboration), Phys. Rev. Lett. **100**, 202001 (2008).

[37] P. Ko, J. Lee, and H. S. Song, Phys. Lett. B **395**, 107 (1997).

[38] C.-F. Qiao, F. Yuan, and K.-T. Chao, Phys. Rev. D **55**, 4001 (1997).

[39] M. Suzuki, Phys. Rev. D **66**, 037503 (2002); P. Colangelo, F. De Fazio, and T. N. Pham, Phys. Lett. B **542**, 71 (2002).

[40] The curves show the signal [large-dashed red line for ψ', short-dashed magenta line for $X(3823)$, and dotted violet line for $X(3872)$] and the background component [dot-dashed black line for combinatorial, two-dot–dashed dark green line for $B \rightarrow \psi'(\nrightarrow \chi_{cJ}\gamma)K$, and cyan three-dot–dashed for peaking component] as well as the overall fit (solid blue line). $B \rightarrow \psi'(\nrightarrow \chi_{cJ}\gamma)K$ is specific to the decay mode under study.